Intramolecular Charge Transfer as Probing Reaction: Fluorescence Monitoring of Protein−Surfactant Interaction

R. Das, D. Guha, S. Mitra, S. Kar,† S. Lahiri,† and S. Mukherjee*

Department of Physical Chemsitry, Indian Association for the Cultivation of Science, Jadavpur, Calcutta-700 032, India

Received: August 20, 1996; In Final Form: January 17, 1997[⊗]

Ethyl *p*-(dimethylamino)cinnamate (EDAC) has been used as a fluorescence probe for monitoring the interaction between a model water-soluble protein, bovine serum albumin (BSA), and an anionic surfactant, sodium dodecyl sulfate (SDS). The probe EDAC undergoes intramolecular charge transfer (ICT) in the excited state in water and other polar solvents. The emission from the ICT state becomes more intense and blue-shifted due to reduced polarity in the hydrophobic environments of BSA and SDS micelles relative to that in pure water. The intensity of the ICT emission from EDAC increases with surfactant concentration and reaches a maximum at the critical micelle concentration of SDS, which can be employed as a simple technique for following micellization. Analysis of the fluorescence spectra of the probe provide evidences in favor of surfactant-induced protein uncoiling due to massive binding of the SDS molecules to BSA in the cooperative binding region of the binding curve, describing protein (BSA)−surfactant (SDS) interaction. The polarity of the BSA−SDS aggregate formed is intermediate between that of hydrophobic regions of BSA and SDS micelles as sensed by the intramolecular charge-transfer (ICT) probe, EDAC.

Introduction

Anionic surfactants, e.g., sodium dodecyl sulfate (SDS) have been well-known for their denaturing action on bovine serum albumin (BSA) and other water-soluble proteins.[1−4] In the native conformation of such a water-soluble protein, BSA, a substantial fraction of the hydrophobic side chains are typically buried in the interior of the molecule. The free energy gained in the process is a major factor in determining the stability of the native conformation in water relative to a more flexible conformation in which the hydrophobic side chains would be exposed to the solvent. So, the protein in its native state, attain a little bit of folded conformation (X, Scheme 2). The denaturation of protein is caused by surfactant-induced unfolding of BSA through binding of SDS to BSA. The native conformation of the protein molecule possesses only marginal stability because it is highly constrained. So, other conformational states, in which a much larger fraction of the hydrophobic side chains is exposed to the solvent than in the native state, are thus readily accessible. Protein molecules in such altered conformational states with many exposed hydrophobic groups are likely to bind a large number of ligands per molecule. The free energy gained thereby may greatly exceed the unfavorable free energy change accompanying the conformational change, and the transition to altered conformational state would then be induced by the presence of the ligand.

However, one of the difficult aspects of the study of protein−surfactant interaction is the determination of the structure of the protein−surfactant complex. The X-ray diffraction studies[5] were unable to visualize about the structure of the protein−surfactant complexes in solution when a large number of surfactant molecules are bound. A variety of models[6] have been proposed for the structure of SDS complexes with BSA and other water-soluble proteins: (a) a model, in which the protein organizes the SDS anions into a "*micelle complex*"; (b) a model based on a "*rodlike*" particle in which the protein forms the backbone of the complex with the SDS bound along the backbone, the particle having a length of 0.074 nm/amino acid residue; (c) a "*pearl-necklace*" model in which the flexible denatured polypeptide chain(s) of the protein has small spherical micelles clustured along it, the transmicellar regions of the polypeptide chains possibly forming α-helix;[6−9] (d) a "*flexible helix*" model in which the SDS forms a flexible cylindrical micelle and the polypeptide chains are chemically wound around it. Some of the most recent works[6−8] have employed the small-angle neutron-scattering technique, and this method is capable of giving much information regarding microstructure of the protein−surfactant complexes. The neutron-scattering data in case of interaction between lithium dodecyl sulfate (LiDS) and BSA were interpreted[7] in terms of a "pearl necklace" structure of protein−surfactant aggregates in which SDS micelles were distributed along the polypeptide chain (Z, Scheme 2).

Molecular spectroscopy has made great advances over recent years in the understanding and description of the photoinduced intramolecular charge-transfer (ICT)[10−14] processes. The molecule of interest here, ethyl *p*-(dimethylamino)cinnamate (EDAC, I, Figure 1) undergoes an intramolecular charge-transfer (ICT) reaction in the first excited singlet state (Scheme 1), in water and other polar solvents, with the resulting ICT emission being sensitive to solvent polarity. Incorporation of molecular probes into aqueous micelles and proteins effectively unravel parameters such as the critical micelle concentration (cmc), degree of water penetration into these surfactant aggregations, and local polarity of the microenvironment of the binding sites of proteins. Studies employing molecular probes[15−17] with fluorescence characteristics are known to reflect their microenvironment. The physical parameters such as fluorescence emission maxima, intensity values, lifetime, polarization, and excitation spectrum act as potential indicators of the features of a probe's surroundings.[15] Selective targetting of specific micellar domains and protein microenvironments have been precisely achieved[18] with fluorophores such as polycyclic aromatic hydrocarbons (pyrene, naphthalene) and with ionic derivatives of aromatic chromophores, e.g., 1-anilinonaphthalene-8-sulfonate (ANS), 2-*p*-

* To whom all correspondence should be addressed,
† Department of Organic Chemsitry, IACS.
⊗ Abstract published in *Advance ACS Abstracts,* May 1, 1997.

S1089-5639(96)02566-2 CCC: $14.00

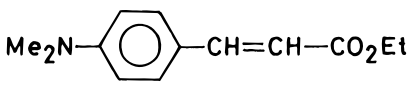

EDAC, I

Figure 1. Ethyl *p*-(dimethylamino)cinnamate (I, EDAC).

SCHEME 1: Schematic Energy State Diagram for the Dynamic Processes of the Excited States of EDAC[a]

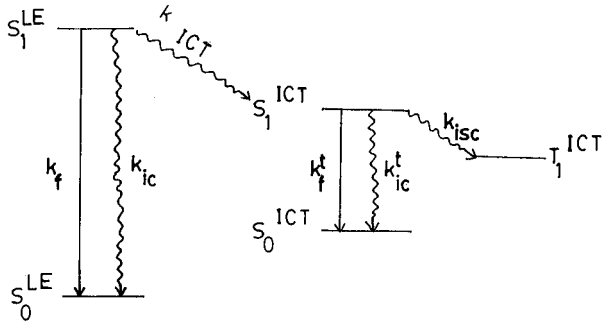

[a] k_{ICT} = rate constant for the ICT process, k_f = radiative rate constant of the locally excited (LE) state, k_{ic} = rate constant for the internal conversion of LE state, k_f^t = radiative rate constant for the ICT state, k_{ic}^t = internal conversion rate of ICT state, k_{isc} = rate constant for intersystem crossing from the ICT state.

toluidinylnaphthalene sulfonate (TNS), etc. However, the probe EDAC (I, Figure 1) is a novel molecular reporter with potential added advantage for following surfactant-induced protein uncoiling as well as micelle formation. This neutral, hydrophobic probe displays appreciable shift in the fluorescence maximum with a variation in solvent, enabling the location of the probe in distinct regions to be established, e.g., emission maxima range from 390 nm in nonpolar cyclohexane to 485 nm in water. Moreover, the fluorescence maxima of the ICT emission of EDAC correlates well with the static polarity of the environment and the intensity of the fluorescence increases with decreasing polarity of the medium. In addition to this spectral sensitivity, EDAC, has the advantage of exhibiting measurable fluorescence intensities in both polar and apolar solvents. Thus, fluorescence signatures from a location of the probe in the bulk solvent as well as within the various microenvironments of a surfactant aggregation and protein are discernible. Both the polarity-dependent spectral shift and fluorescence intensity variation enable the fluorescence contributions from multiple populations of probe molecules to be easily resolved.[19,20] A further advantage of EDAC over other common probes such as ANS, TNS is the absence of a permanent charge, which eliminates complications originating from ionic interactions.[19]

Two features act in the added advantage for EDAC as a fluorescence probe: (i) it is neutral and hydrophobic; (ii) its emission maxima correlate quite excellently with static polarity of the environment, in terms of an empirical solvent polarity parameter, $E_T(30)$.[21] Since EDAC is neutral and hydrophobic, it may be solubilized in the protein−surfactant aggregate when protein−surfactant interaction has been completed, although some probe molecules are expelled to the bulk aqueous phase. As a result, the local polarity of the protein−surfactant aggregate formed due to protein surfactant interaction can be estimated from emission spectra of EDAC under proper conditions, due to the good correlation between fluorescence maxima of EDAC and static polarity of the environment, which is also the case for ionic probes such as ANS, TNS.[22,23] However, in case of ionic fluorophores such as ANS, TNS, etc., these hydrophilic probes possessing an anionic sulfonate group are expected to be expelled to the bulk aqueous phase when protein−surfactant interaction is complete and there is no possibility of these ionic probes for being solubilized in the BSA−SDS aggregate. Thus, the possibility of estimation of micropolarity of BSA−SDS aggregate becomes much less feasible with these ionic fluorophores. So, apart from following surfactant-induced protein uncoiling, EDAC can also be used as a "polarity sensor" for the protein−surfactant aggregate.

The advantage of using EDAC over some other neutral, hydrophobic probes, e.g., pyrene is that in EDAC photoinduced intramolecular charge transfer (ICT) takes place in the excited singlet state resulting in an excellent correlation between the emission maxima of EDAC and static polarity of the environment, and thus the micropolarity of the BSA−SDS aggregate can be expressed quantitatively in terms of an empirical solvent polarity parameter, $E_T(30)$.[21] In case of pyrene the fluorescence intensities for various vibronic fine structures show strong solvent dependence. In polar solvents, there is a significant enhancement in the intensity of the 0−0 vibronic band at the expense of other bands. In effect the ratio of the third to the first fluorescence band of pyrene monomer is found to be sensitive to medium polarity.[24] This strong perturbation in the vibronic band intensities is more dependent on the solvent dipole moment than on the bulk solvent dielectric constant; the major contributions to vibronic band intensities is from some specific solute−solvent dipole−dipole coupling mechanism rather than a universal interaction due to the collective influence of the solvent as a dielectric medium. The mechanism involving the latter path are fairly well understood and explained in terms of static polarity of the solvent. Thus, the local polarity of an environment cannot be expressed quantitatively in terms of an empirical solvent polarity parameter, using pyrene as probe. These features of the probe is very useful in investigating structural transitions in a biopolymer like BSA, e.g., as a monitor of protein unfolding induced by surfactants.

The present research deals with the application of this probe for following *(i) micellization of surfactant and (ii) surfactant-induced protein uncoiling as well as (iii) a polarity sensor for the determination of micropolarity of protein−surfactant aggregates.*

We have also separately determined a binding curve of SDS to BSA (Figure 2) and compared the results of the binding curve with that of fluorescence measurements of EDAC, to check the validity of "*fluorescence probe*" technique in following the SDS−BSA interaction. In constructing the binding curve for the interaction between BSA and SDS, we have followed the change in intrinsic fluorescence of BSA, on addition of SDS.

Materials and Methods

Ethyl *p*-(dimethylamino)cinnamate (EDAC) is prepared from *p*-(dimethylamino)benzaldehyde by the standard procedure.[25] The compound is purified by column chromatography followed by repeated crystallization from ethanol. Bovine Serum Albumin (99%) was obtained from Sigma Chemical Co. and used as received. Triply distilled water was used throughout this study. Sodium dodecyl sulphate (SDS) was obtained from Aldrich Chemical Co. and purified by washing with ether followed by repeated recrystallization from the ethanol/ether mixture. All the solutions were prepared in a sodium phosphate buffer (pH = 7). The sample concentrations for EDAC were maintained at 1×10^{-5} mol dm^{-3}. Steady-state absorption and emission spectra were recorded with a JASCO (UV/vis) Model 7850 and Perkin Elmer MPF 44B spectrophotometers, respectively.

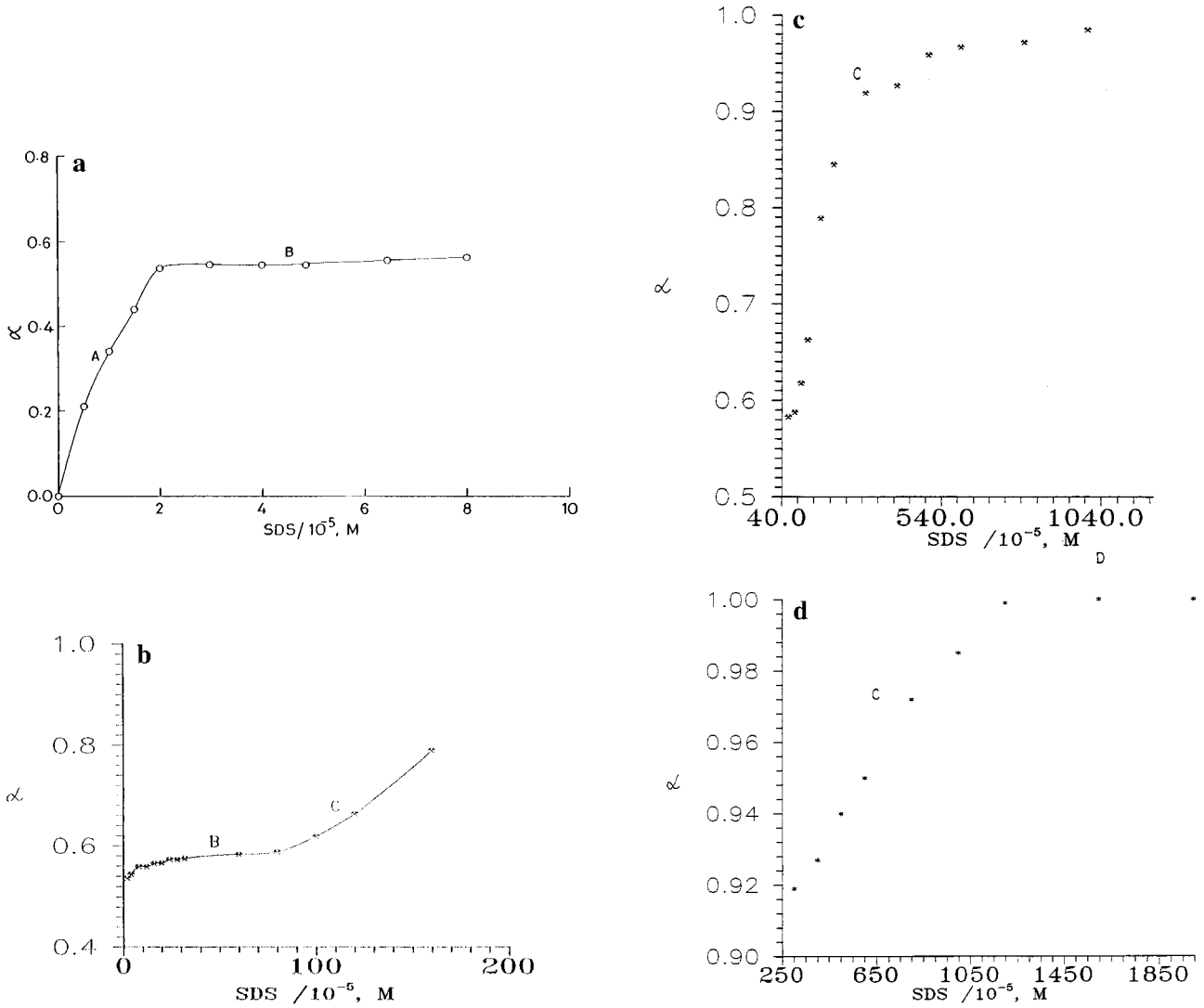

Figure 2. Binding curve (α vs [SDS]) showing interaction between BSA and SDS; [BSA] = 30 μM, in a phosphate buffer solution of pH 7, ionic strength = 0.014, α = fraction of a BSA molecule bound by SDS.

Results and Discussion

1. Binding Curve for BSA−SDS Interaction. The nature of the BSA−SDS interaction can be well understood in terms of binding curve or binding isotherm.[4,26] Figure 2 shows the binding curve for the BSA−SDS interaction. In the binding curve, fractions (α) of a BSA molecule bound by SDS have been plotted as a function of total SDS (bound + free) concentration.

If a BSA molecule possess n_0 number of binding sites and at a certain stage SDS molecules bind to n number of such sites, then the fraction of a BSA molecule bound to SDS is $\alpha = n/n_0$. At the saturation binding condition, when all the possible sites of BSA are occupied/bound by SDS, $\alpha = 1$ and after that no further interaction between BSA and SDS takes place. So, in the absence of SDS, $\alpha = 0$ and when BSA−SDS complexation has been completed and no further surfactant protein interaction occurs, $\alpha = 1$. The binding characteristics in Figure 2 identify four regions (A, B, C, D) and is similar to that observed by previous workers.[2,4,26] Initially at region A (Figure 2a) binding of some SDS molecules occur on specific high energy sites of BSA at very low concentration of SDS. The slow-rising part after region A is region B, which is followed by a third region C, Figure 2b,c and is termed as the cooperative binding region. In this region, a massive increase in binding of SDS to BSA takes place because of cooperative interactions resulting in SDS-induced unfolding of BSA. Beyond region C, a plateau (region D, $\alpha = 1$) is observed (Figure 2d), suggesting that further binding of the surfactant does not occur on the protein. Region D is termed as the saturation binding region.

2. Fluorescence Solvatochromism of Ethyl *p*-(Dimethylamino)cinnamate (EDAC) and Intramolecular Charge Transfer (ICT). The fluorescence emission spectra of EDAC is found to be polarity-dependent. In water it exhibits a small Stokes-shifted emission at 407 nm and large Stokes-shifted emission maxima at 485 nm. This large Stokes-shifted emission at 485 nm is progressively blue shifted with decreasing polarity of the solvent and in acetonitrile (ACN) the emission maxima is observed at 450 nm (Figure 3). However, the absorption maxima is almost independent of solvent polarity (λ_{abs}^{ACN} = 358 nm, λ_{abs}^{water} = 361 nm). These observations can be successfully explained by assuming that the polarity-dependent emission originates from the charge-transfer character of the emissive state.

In EDAC, a charge separation in the excited state may result from the transfer of an electronic charge upon excitation from a donor (D) to an acceptor (A) site. The acceptor part is made up of a benzene ring and of a para group (−CH=CHCO$_2$Et) and donor part is a dimethylamino (NMe$_2$) group as shown in Figure 1. The two moieties are flexibly linked by the C−N bond. According to our AM1 calculations[27] the ground state

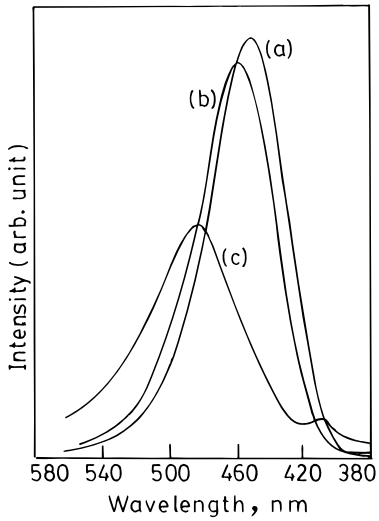

Figure 3. Emission spectra of EDAC in (a) acetonitrile, (b) *N*,*N*-dimethyl sulfoxide, and (c) water; $\lambda_{exc} = 358$ nm.

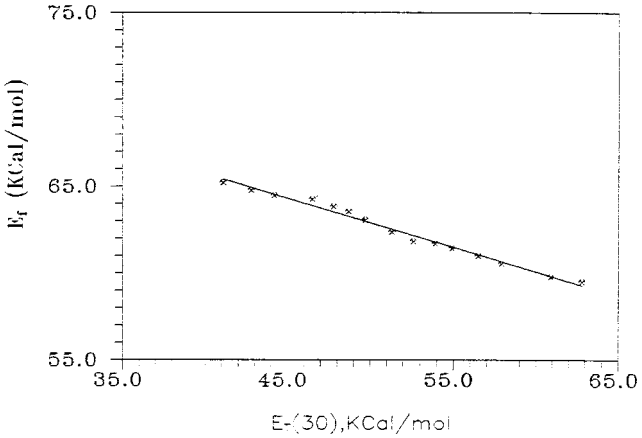

Figure 4. Plot of fluorescence energy (kcal/mol) of EDAC vs $E_T(30)$ of different water−dioxane mixtures.

and Franck−Condon (FC) or locally excited (LE) state of EDAC is nonplanar. The stereochemistry at the dimethylamino nitrogen atom is pyramidal in the ground state. Upon excitation the pyramidal dimethylamino group undergoes a twist around the C−N bond which results in a nearly coplanar geometry for EDAC in the first excited state facilitating further delocalization of electron density into the aromatic ring. The results of detailed calculations will be described elsewhere.[27] This process may be called *intramolecular charge transfer*,[14] and the resulting state may be labeled as an *ICT state* (Scheme 1) in comparison to the *twisted intramolecular charge transfer (TICT)* model proposed by Grabowski[13] et al. In the original TICT proposed by Grabowski et al. the nearly coplanar dimethylamino group is twisted to the conformation perpendicular to the phenyl ring in order to facilitate the complete charge separation in the excited singlet state leading to the large stabilization due to the interaction with polar solvents.

Due to its charge-transfer character, the ICT state is modified by solvent stabilization and polarity-dependent ICT emission is observed for this molecule (Figure 3). The emission maxima of the ICT state (in terms of fluorescence energy in kcal/mol) shows an excellent linear correlation (Figure 4) with an empirical solvent polarity parameter, $E_T(30)$[21] in water−dioxane mixtures. The ICT emission is increasingly red-shifted with increasing polarity of the solvent, as the energy gap ΔE ($S_1^{ICT}-S_0^{ICT}$) between ground and excited states decreases (Scheme 1) with increase in solvent polarity.

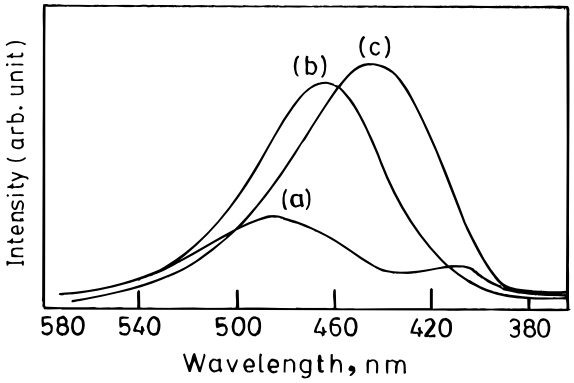

Figure 5. Emission spectra of EDAC in (a) pure water, (b) 9 mM SDS, and (c) 30 μM BSA; $\lambda_{exc} = 358$ nm.

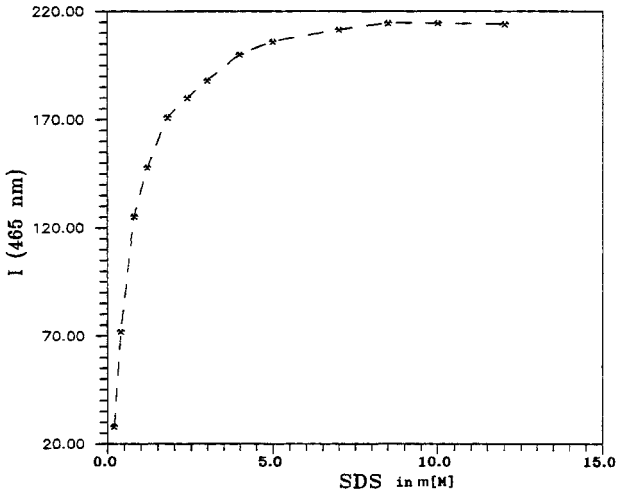

Figure 6. Plot of ICT fluorescence intensity at 465 nm, I (465) vs SDS concentration in mM.

3. Steady-State Fluorescence Spectra of EDAC in BSA and SDS Micelles. In water, a weak ICT emission of EDAC is observed at 485 nm. But this ICT emission is blue-shifted to 443 and 465 nm in aqueous BSA and SDS solutions, respectively, with a strong enhancement in fluorescence intensity (Figure 5). These observations clearly show that EDAC is solubilized in the hydrophobic regions of the protein and surfactant. The polarity of these hydrophobic regions are much less than that of the pure aqueous phase as seen from the blue-shifted emission spectrum.

3.1. Determination of Critical Micelle Concentration (cmc) of SDS. The fluorescence spectra of EDAC exhibits a marked change on addition of SDS. As seen from Figure 6 the intensity of the ICT emission increases with surfactant concentration and reaches a maximum at the critical micelle concentration of the surfactant. The cmc of SDS determined from the data in Figure 6 is 8.5 mM, which agrees quite well with the reported values.[24] Thus, the ICT probe EDAC offers a simple technique for determining the cmc of an anionic surfactant.

The increase in intensity of the ICT emission of probe molecule, EDAC as well as the corresponding blue-shift in SDS micelles relative to that in pure water is accounted for by the following plausible reasons: (1) During the formation of micellar aggregates the EDAC molecules are transferred from the highly polar aqueous phase to the less polar and hydrophobic micellar environment. The singlet excited ICT state is much more polar than the corresponding singlet ground ICT state, because the dipole moment of the molecule in the singlet excited ICT state, $\mu(S_1^{ICT})$, and dipole moment of the molecule in the ground singlet ICT state, $\mu(S_0^{ICT})$, are estimated to be 8.84 and

5.23 D, respectively, from our AM1 calculations.[27] Therefore, the ICT state (S_1^{ICT}) becomes relatively less stabilized than the corresponding ground state in the less polar hydrophobic interior of SDS micelles than in pure water. This results in an increase in the energy gap, $\Delta E(S_1^{ICT}-S_0^{ICT})$ between the S_1 and S_0 states (Scheme 1) with a consequent blue-shift in the ICT emission. In consequence of this increase of $\Delta E(S_1^{ICT}-S_0^{ICT})$ in the hydrophobic interior of micelles than in pure water, the rate of nonradiative deactivation (internal conversion) from S_1^{ICT} to S_0^{ICT} is higher in pure water than in the less polar hydrophobic interior. This fact accounts for the stronger ICT emission in the hydrophobic environment relative to that in pure water.

(2) Moreover, due to this reason the rate of nonradiative deactivation of the singlet ICT state to the triplet ICT state (intersystem crossing) significantly decreases resulting in an enhanced ICT emission (Scheme 1). This is because the rate of nonradiative transition from the S_1 state to the T_1 state decreases exponentially with an increase in S_1-T_1 energy gap.[28] Our theoretical calculations using the AM1 technique also support this reasoning. The dipole moment of the first excited singlet state, $\mu(S_1^{ICT})$, and the first excited triplet state, $\mu(T_1^{ICT})$, are evaluated to be 8.84 and 8.31 D, respectively. Thus, relaxation by low-polarity solvent would therefore be expected to increase the singlet−triplet energy split, hindering intersystem crossing (isc) and thereby enhancing the ICT fluorescence.

(3) Another important point[29] is that water quenches the fluorescence of EDAC due to the radiationless transitions induced by hydrogen-bonding interactions. E.g., in the case of dyes[30] stronger hydrogen-bonding solvents have been found to cause a larger rate of singlet-to-triplet intersystem crossing. In consequence a weak ICT emission of EDAC is observed in pure water. Due to the formation of micelles, the EDAC molecules are transferred from the highly polar aqueous phase to a less polar hydrophobic micellar environment. As a result, the solute−solvent hydrogen-bonding interactions in pure water, between probe EDAC and water, are perturbed in a micellar environment. This perturbation of the solute−solvent hydrogen-bonding interactions causes diminution of radiationless transitions (induced by hydrogen-bonding interactions) for EDAC in micellar environment with a resultant enhancement of ICT emission in SDS micelles.

Similar reasonings hold well for the blue-shifted and stronger ICT emission of EDAC in BSA solution. Here, the EDAC molecules are transferred from the highly polar aqueous phase to the less polar hydrophobic regions of BSA.

Thus it is evident from Figure 5 that the ICT emission of EDAC gets enhanced with increasing hydrophobicity of the surrounding environment, and the intensity of the ICT emission can be used as an index of hydrophobicity of the environment in which the probe molecule is solubilized.

3.2. Surfactant-Induced Changes in Fluorescence Spectra of EDAC in BSA. The fluorescence spectra of EDAC in aqueous BSA solution shows a maximum at 443 nm. On addition of SDS, the emission maxima at 443 nm is red-shifted to 454 nm. The plot of emission intensity at 454 nm vs SDS concentration is shown in Figure 7. The results in Figure 7a,b show that at first there is an increase in intensity followed by a reduction and then a sharp increase beyond a certain concentration of SDS (0.8 mM). These observations suggest that hydrophobicity of the region in which the probe is localised varies as the binding curve (Figure 2) along SDS concentration, [SDS] is traversed. The initial increase in the intensity is attributed to the cobinding of the surfactant and probe molecules near the hydrophobic regions of the protein. The reduction in intensity originates due to the release of some of the probe molecules into a more

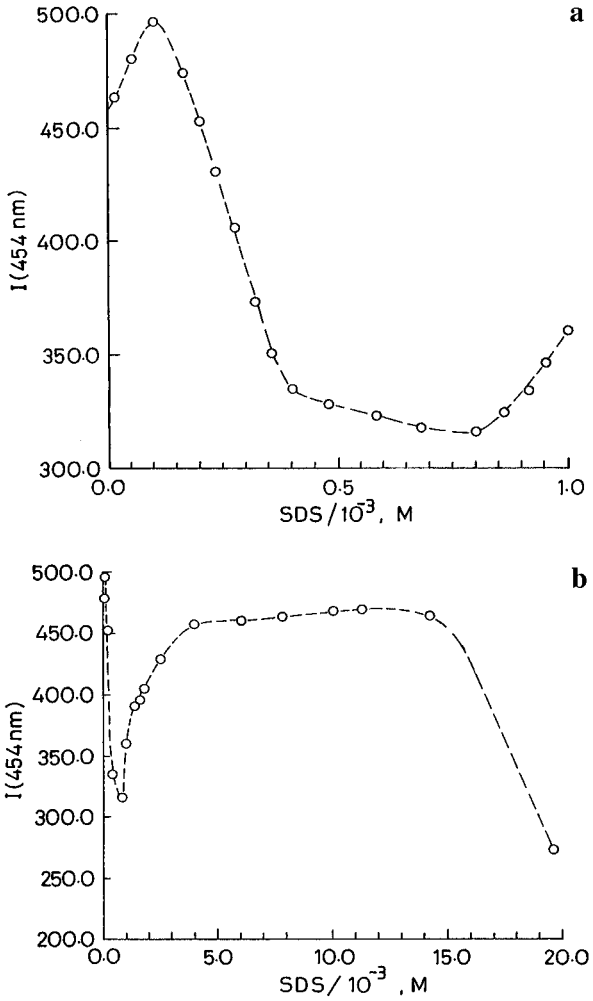

Figure 7. Variation of emission intensity (at 454 nm) of EDAC bound to BSA in presence of SDS.

SCHEME 2: Schematic Presentation of Surfactant (SDS) Induced Uncoiling of Protein (BSA)

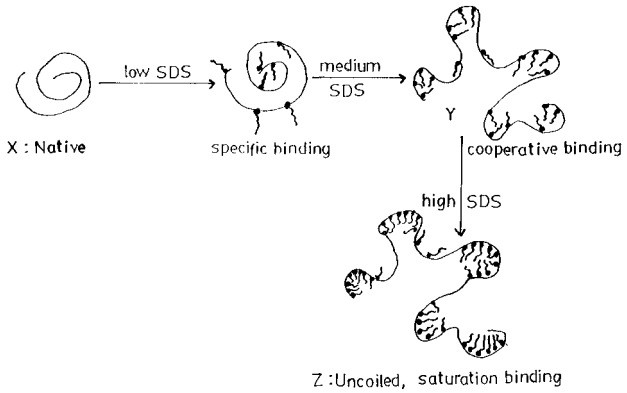

hydrophilic phase because of the competetion for binding with SDS to the protein molecule. Beyond the minimum, the intensity of the ICT emission of the probe molecule increases at a SDS concentration of 0.8 mM (Figure 7b). It is quite interesting to note that this observation corresponds closely to the onset of a sharp rise in the binding curve (Figure 2b) indicating that in this region massive binding of the surfactant begins to occur on the protein leading to its uncoiling. As the protein goes from its native coiled state (X) to uncoiled state (Y, Scheme 2), the number of hydrophobic binding sites markedly increases. Therefore, the probe (EDAC) molecules get increasingly solubilized in the hydrophobic regions due to surfactant-induced protein unfolding. Hence, the intensity of

emission at 454 nm increases as the probe senses increasing hydrophobicity of its surrounding environment. It is also quite evident from Figure 7b that at 11.5 mM of SDS, the intensity of emission reaches a maximum. This observation indicates that at this SDS concentration, surfactant-induced unfolding of BSA becomes complete and no further binding of SDS occurs on BSA above this concentration. The probe EDAC is solubilized in the hydrophobic regions of SDS−BSA aggregate. At a much higher level of SDS concentration at 20 mM, the intensity of 454 nm emission decreases probably because SDS expels some probe molecules bound by hydrophobic interactions to the SDS−BSA aggregate, into the bulk aqueous phase.

3.3. Estimation of Micropolarity of the Hydrophobic Regions of BSA−SDS Aggregate: EDAC as a Polarity Sensor. The charge-transfer character of the ICT emissive state of EDAC and accompanying fluorescence solvatochromism (Figures 3 and 4) features it as a *polarity sensor* for an environment where it is localized/solubilized.

However, despite addition of 20 mM SDS (Figure 7b) to aqueous BSA solution containing EDAC, some probe molecules remain localized in the hydrophobic SDS aggregates bound to protein, and the polarity of these aggregates appears to be greater than the hydrophobic regions of SDS-free BSA but less than that of SDS solution. This is because the ICT emission in pure BSA and SDS solutions are at 443 and 465 nm, respectively (Figure 5), while the ICT emission in BSA−SDS aggregate is observed at 454 nm. The polarity of the hydrophobic interior of BSA, SDS micelles, and BSA−SDS aggregates have been estimated in terms of a solvent polarity parameter, $E_T(30)$ from a comparison of the emission maxima of EDAC solubilized in these regions with those of EDAC in aqueous dioxane−water mixtures (Figure 4). From such a comparison the $E_T(30)$ values for pure BSA, pure SDS micelles and BSA−SDS aggregates are found to be 43.5, 54.4, and 49.7, respectively.

4. Comparison of Steady-State Results with That of the Binding Curve. The SDS-induced changes in the fluorescence spectra of EDAC bound to hydrophobic regions of BSA indicates the onset of cooperative binding region at 0.8 mM of SDS, which exactly coincides with that of the onset of region C at 0.8 mM SDS concenration of the binding curve (Figure 2b). The fluorescence spectra indicates saturation binding of SDS to BSA at 11.5 mM SDS concentration (Figure 7b). However, the binding curve (Figure 2d) indicates the onset of saturation binding region at [SDS] = 12 mM. Thus, the results of fluorescence probe analysis agrees quite well with that of the binding curve results.

Conclusions

Fluorescence probe analysis as well as the binding curve results suggest that (1) the critical micelle concentration of SDS in pure water is 8.5 mM and (2) at low concentration of SDS, the binding of surfactant molecules occurs at specific sites of protein through ionic interactions (Scheme 2). This is in the initial region A of the binding curve (Figure 2a) describing protein−surfactant interaction. This sort of specific binding causes small expansion of the protein molecule leading to noncooperative binding (which corresponds to the slow rising part B of Figure 2b). On addition of further SDS, massive binding of surfactants to protein take place due to cooperative interactions (Figure 2c and Scheme 2). This is in the cooperative binding region of the binding curve. The massive cooperative binding leads to uncoiling of BSA and exposure of a significant number of hydrophobic binding sites previously buried in the interior of BSA. This unfolding of the protein molecule promotes formation of micelle-like aggregates by wrapping around them (Z, Scheme 2). This is known as "*pearl necklace*" model for the surfactant−protein complex.

(3) The polarity of this BSA−SDS aggregate is intermediate between that of the hydrophobic regions of protein and micelle and is equivalent to a homogeneous water−dioxane mixture with $E_T(30) = 49.7$.

Acknowledgment. R.D. and S.M. are grateful to the Council of Scientific and Industrial Research, Government of India for providing them with research fellowships.

References and Notes

(1) Steinhardt, J.; Reynolds, J. A. In *Multiple Equlibria in Proteins*; Academic Press: New York, 1969.
(2) Tanford, C. In *The Hydrophobic Effect: formation of micelles and biological membranes*, 2nd ed., Wiley-Interscience: New York, 1986; Chapter 14.
(3) Jones, M. N. *Biochem. J.* **1975**, *151*, 109.
(4) Schwuger, M. J.; Bartnik, F. G. In *Anionic Surfactants*; Gloxhuber, C., Ed.; *Surfactant Science Series*, Vol. 10; Marcel Dekker: New York, 1980; Vol. 10, Chapter 1.
(5) Yonath, A.; Podjarny, A.; Honig, B.; Sielecki, A.; Traub, W. *Biochemsitry* **1977**, *16*, 1418.
(6) Ibel, K.; May, R. P.; Kirschner, K.; Szadkowski, H.; Mascher, E.; Lundahl, P. *Eur. J. Biochem.* **1990**, *190*, 311.
(7) Chen, S. H.; Teixeira, J. *Phys. Rev. Lett.* **1986**, *57*, 2583.
(8) Guo, X. H.; Zhao, N. M.; Chen, S. H.; Teixeira, J. *Biopolymer* **1990**, *29*, 335.
(9) Shirahano, K.; Tsujii, K.; Takagi, T. *Biochem. J.* **1974**, *75*, 309.
(10) Rettig, W. *Angew Chem., Int. Ed. Engl.* **1986**, *25*, 971.
(11) Mataga, N.; Yao, H.; Okada, T.; Rettig, W. *J. Phys. Chem.* **1989**, *93*, 3383.
(12) Simon, J. D.; Su, S. *J. Phys. Chem.* **1988**, *92*, 2395.
(13) Grabowski, Z. R.; Rotkiewicz, K.; Siemiarczuk, A. *J. Lumin.* **1979**, *18/19*, 420.
(14) Gorse, A.-D.; Pesquer, M. *J. Phys. Chem.* **1995,** *99*, 4039 and references therein.
(15) Azzi, A. *Q. Rev. Biophys.* **1975**, *8*, 237.
(16) Dodiuk, H.; Kanety, H.; Kosower, E. M. *J. Am. Chem. Soc.* **1979**, *83*, 515.
(17) Das, R.; Mitra, S.; Nath, D. N.; Mukherjee, S. *J. Phys. Chem.* **1996**, *100*, 14514.
(18) Gratzel, M.; Thomas, J. K. In *Modern Fluorescence Spectroscopy 2*; Wehry, E. L., Ed.; Plenum Press: New York, 1976; Chapter 4.
(19) Weber, G.; Farris, F. J. *Biochemistry* **1979**, *18*, 3075.
(20) Torgenson, P. M.; Drickamer, H. G.; Weber, G. *Biochemistry* **1977**, *18*, 3079.
(21) Reichhardt, C. *Chem. Soc. Rev.* **1992**, *21*, 147.
(22) Kosower, E. M. *Acc. Chem. Res.* **1982**, *15*, 259.
(23) Kosower, E. M.; Dodiuk, H.; Kanety, H. *J. Am. Chem. Soc.* **1978**, *100*, 4179.
(24) Kalayanasundaram, K.; Thomas, J. K. *J. Am. Chem. Soc.* **1977**, *99*, 2039.
(25) Vogel, A. In *Textbook of Practical Organic Chemsitry*, 4th ed.; ELBS, 1978; p 535.
(26) Reynolds, J. A.; Tanford, C. *Proc. Natl. Acad. Sci. U.S.A.* **1970**, *66*, 1002.
(27) Mitra, S.; Das, R.; Mukherjee, S., to be communicated.
(28) Avouris, P.; Gelbert, W. M.; El-Sayed, M. A. *Chem. Rev.* **1977**, *77*, 793.
(29) Thanks to the reviewer, for suggesting and drawing our attention to this point. This effect should be taken as a general mechanism in addition to the change of the energy gap in polar or less polar environments.
(30) Cramer, L. E.; Spears, K. G. *J. Am. Chem. Soc.* **1978,** *100*, 221.